Supporting Information for:

The Role of the Secondary Coordination Sphere in a Fungal Polysaccharide Monooxygenase

Elise A. Span[1], Daniel L. M. Suess[2], Marc C. Deller[3], R. David Britt[2], Michael A. Marletta[4,5,*]

[1] Biophysics Graduate Group, University of California, Berkeley, Berkeley, CA 94720
[2] Department of Chemistry, University of California, Davis, Davis, California 95616
[3] The Joint Center for Structural Genomics, The Scripps Research Institute, La Jolla, CA 92037
[4] Department of Chemistry, University of California, Berkeley, Berkeley, CA 94720
[5] Department of Molecular and Cell Biology, University of California, Berkeley, Berkeley, CA 94720
*Corresponding author: marletta@berkeley.edu

Supplemental text.

Structure of *Mt*PMO3*.

*Mt*PMO3* exhibits an overall β-sandwich fold resembling fibronectin type III (FnIII) or immunoglobulin (Ig) domains, similar to previous PMO structures, and consists of two β-sheets formed by an anti-parallel arrangement of nine total β-strands (Figure 1a, main text). The rest of the structure is made up of extensive loop regions, many of which exhibit high crystallographic B-factors (~50%), indicating disorder. Two disulfide bonds (Cys48–Cys172 and Cys 87–Cys94) anchor smaller loop features to the β-sandwich. The active site is located in the center of a flat substrate-binding surface (~500 Å^2). Deviations from expected disulfide bond lengths and Cu(II) coordination geometries strongly imply that X-ray induced photoreduction occurred during data collection. The estimated diffraction-weighted X-ray dose was ~10 MGy[1], which exceeds the doses (~1 MGy) observed to reduce Cu centers in bacterial PMOs[2].

The polypeptide chains (A–F) exhibit overall good agreement with each other and result in a pairwise C_α RMSDs <0.2 Å over all 228 residues. The amino acids of each chain are numbered according to the sequence of the mature polypeptide (translated from gene ID MYCTH_92668), beginning with the *N*-terminal histidine residue (*i.e.* H1). The most *C*-terminal ten residues of each chain were not modeled due to a lack of observable electron density.

The LS loop of chain D was best modeled in a slightly different conformation than that of the other five chains; it also exhibits poor electron density for some residues and contains outliers for both Real-space R-value Z-scores (RSRZ) (T115) and Ramachandran analyses (D112). These discrepancies are due to a crystal packing artifact in which the carboxylate moiety of D112 extends to form a H-bond with D13 and T69 residues on chain F, thereby distorting the rest of the LS loop of chain D. The final structure contains additional Ramachandran outlier prolines or proline adjacent residues (P33, D34, P170) that appear necessary to accommodate the unique stereochemical constraints of these proline side chains.

Compared to other structures of fungal, cellulose-active PMOs, the structure of *Mt*PMO3* does not display any significant structural differences in the polypeptide main chain. The largest structural deviations occur in the LS and L2 loops; the latter is believed to vary according to reaction regioselectivity in the AA9 enzymes. In PMO3 enzymes that form both C1 and C4 oxidation products, the L2 loop is large and contains an α-helical segment of 5–11 residues; in *Mt*PMO3* the L2 loop is abbreviated by 5–8 residues and lacks the α-helix (Supplementary Figure 4). This result is consistent with a previous experiment in which the L2 loop of a PMO3 was deleted, resulting in a loss of C4-oxidized products, but retention of C1 activity[3].

One notable difference from previous PMO structures is that the side chain of H161 swings "out" rather than "in" towards the Cu in four of the six molecules in the asymmetric unit (*i.e.* chains A, B, D, and F adopt an "out" conformation). This unprecedented rotamer is stabilized by weak H-bonds with Q162 and E121 on the LS loop, which is longer in *Mt*PMO3* and extends closer to the active site when compared with other AA9 enzymes. In most chains there is weak difference electron density for the other, "inward-facing" rotamer, and the loop containing H161 (here termed L8) exhibits higher-than-average B-factors, indicating general disorder in this region. In the remaining two molecules (chains C

and E), H161 swings “in” towards the Cu and appears trapped in that conformation by a H-bonding interaction with D26 from a symmetry-related molecule within the crystal (Figure 2a, main text). Interestingly, a recent PMO structure also reported an aspartate from a neighboring molecule crossing over into the active site to coordinate with the Cu ion (coordination via the aspartate carboxylate O atoms which are 2.2 and 2.7 Å away)[4]. In contrast, the carboxylate moiety of D26 is 4.6 Å away from Cu in the *Mt*PMO3* structure.

Supplemental References.

1. Paithankar, K. S.; Garman, E. F., Know your dose: RADDOSE. *Acta Crystallogr D Biol Crystallogr* **2010,** *66* (Pt 4), 381-8.

2. Gudmundsson, M.; Kim, S.; Wu, M.; Ishida, T.; Momeni, M. H.; Vaaje-Kolstad, G.; Lundberg, D.; Royant, A.; Stahlberg, J.; Eijsink, V. G.; Beckham, G. T.; Sandgren, M., Structural and Electronic Snapshots during the Transition from a Cu(II) to Cu(I) Metal Center of a Lytic Polysaccharide Monooxygenase by X-ray Photoreduction. *J. Biol. Chem.* **2014,** *289* (27), 18782-18792.

3. Vu, V. V.; Beeson, W. T.; Phillips, C. M.; Cate, J. H.; Marletta, M. A., Determinants of regioselective hydroxylation in the fungal polysaccharide monooxygenases. *J. Am. Chem. Soc.* **2014,** *136* (2), 562-5.

4. Tan, T. C.; Kracher, D.; Gandini, R.; Sygmund, C.; Kittl, R.; Haltrich, D.; Hallberg, B. M.; Ludwig, R.; Divne, C., Structural basis for cellobiose dehydrogenase action during oxidative cellulose degradation. *Nature communications* **2015,** *6*, 7542.

Supplemental Figures.

Data collection:	
Beamline	SSRL 12–2
Wavelength (Å)	0.9795
Space group	$P2_1$
Unit cell dimensions	
a, b, c (Å)	70.94, 134.30, 79.40
α, β, γ (˚)	90.00, 92.92, 90.00
Resolution	48.74–2.45 (2.52–2.45)
Rsym (%)	0.139
I/σ	9.6 (2.0)
No. reflections	50966
Completeness (%)	98.36 (94.74)
Redundancy	4.6 (4.2)
Refinement:	
Rwork/Rfree	0.1626/0.2086 (0.249/0.289)
No. residues	
Protein	1368
Ligand/Ion	6
Water	295
Average B-factor	36.5
RMSD	
bond length	0.011
bond angle	1.379
Ramachandran	
favored (%)	96.7
allowed (%)	2.65
outliers (%)	0.66

Supplementary Table 1. Crystallographic data collection and refinement statistics.

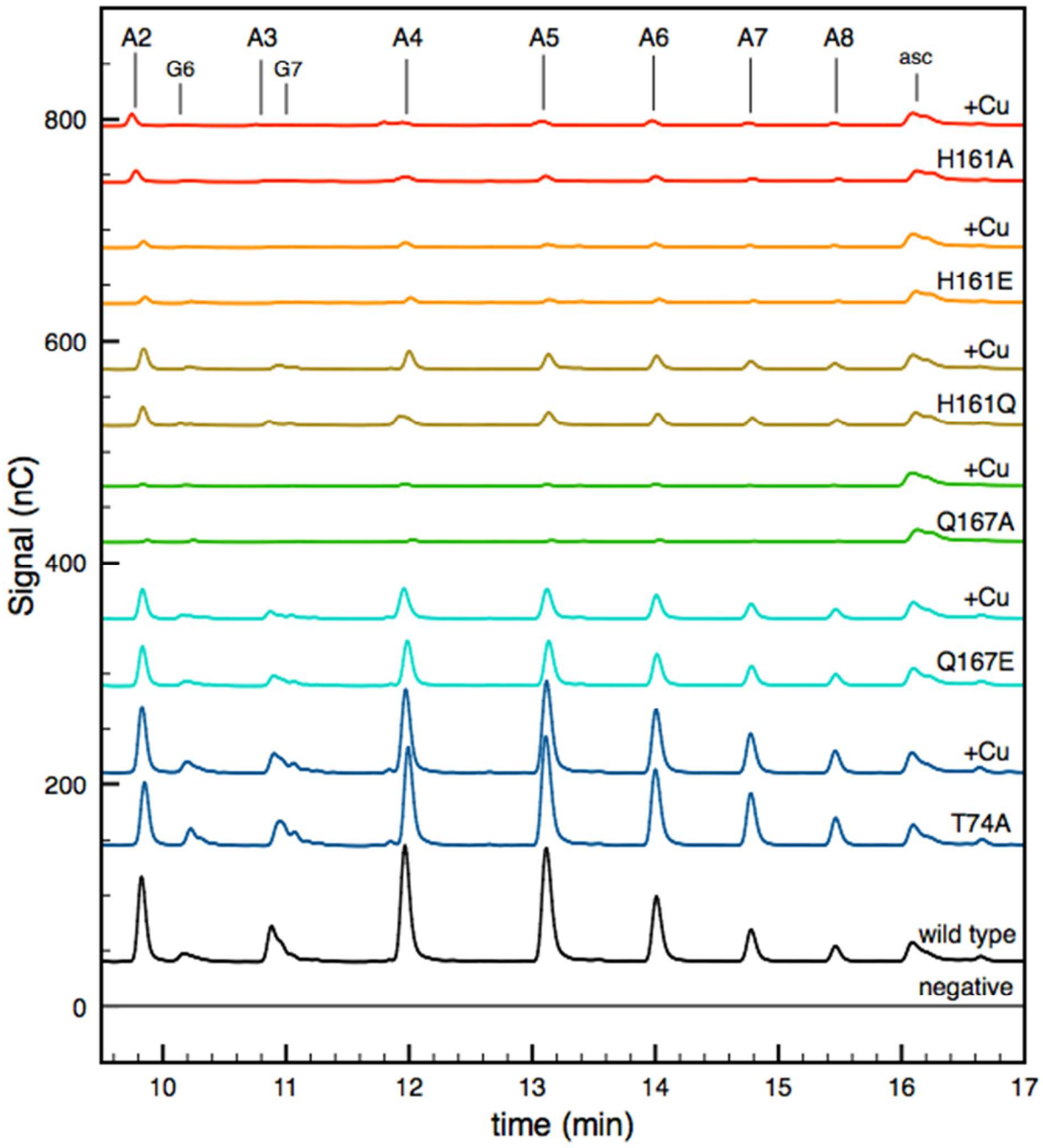

Supplementary Figure 1. PASC activity assays with and without exogenous Cu(II) added (5 µM) to the reactions. Assays (60 µL) contained 5 µM PMO, 5 mg/mL PASC, atmospheric O_2, and 2 mM ascorbate as the reducing agent. Reactions were carried out in 50 mM sodium acetate buffer (pH 5.0) at 42 ˚C for 2 hours.

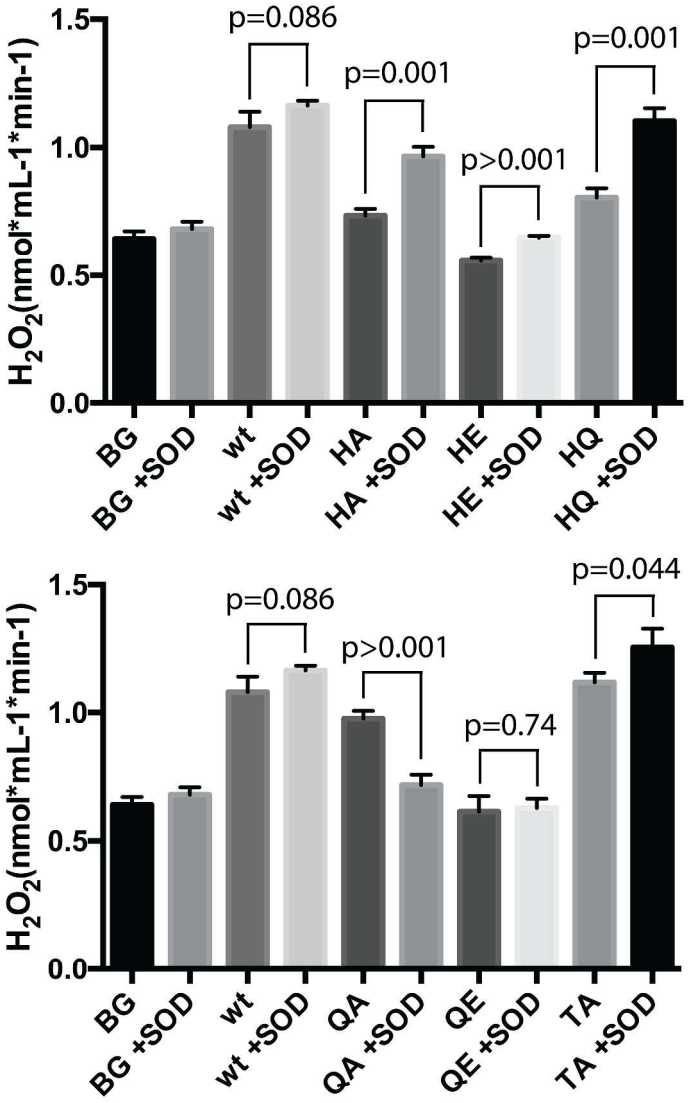

Supplementary Figure 2. Horseradish peroxidase (HRP)-coupled assays ± superoxide dismutase (SOD) with *Mt*PMO3* variants. Assays were carried out in 100 uL of 100 mM HEPES pH 7.0 and contained 0.5 µM PMO, 0.5 U/mL HRP, 50 µM Amplex Red, 0.5 µM MtCDH-2, 100 µM cellobiose, and ± 25 U/mL SOD. BG = background, without PMO. (n=3)

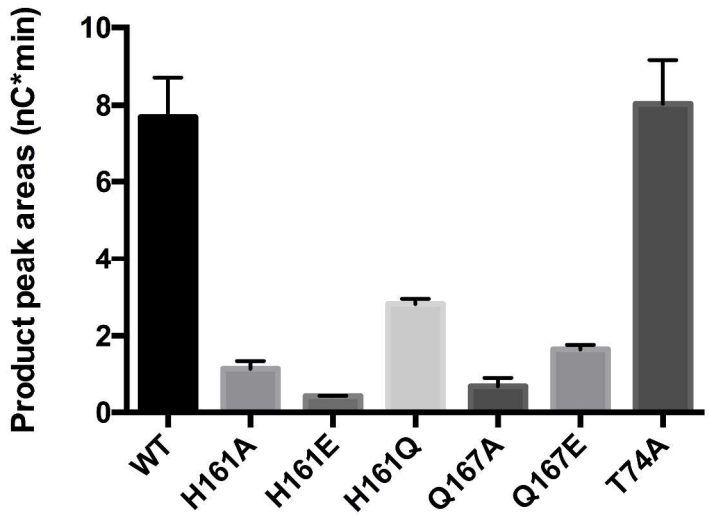

Supplementary Figure 3. Thirty-minute PASC assays showing effect of H-bonding network substitutions on *Mt*PMO3* activity. Assays contained 2 μM PMO, 10 mg/mL PASC, atmospheric O_2, and 1 μM *Mt*CDH-2 as the reducing agent. Reactions of 45 μL were carried out in 50 mM sodium acetate buffer (pH 5.0) at 40 ˚C for 30 minutes. Peaks from aldonic acids with DP 5–13 were quantified via HPAEC. Smaller C1-oxidized products with DP 2–4 were excluded from this analysis, as they are also products of the CDH reaction. (n=3)

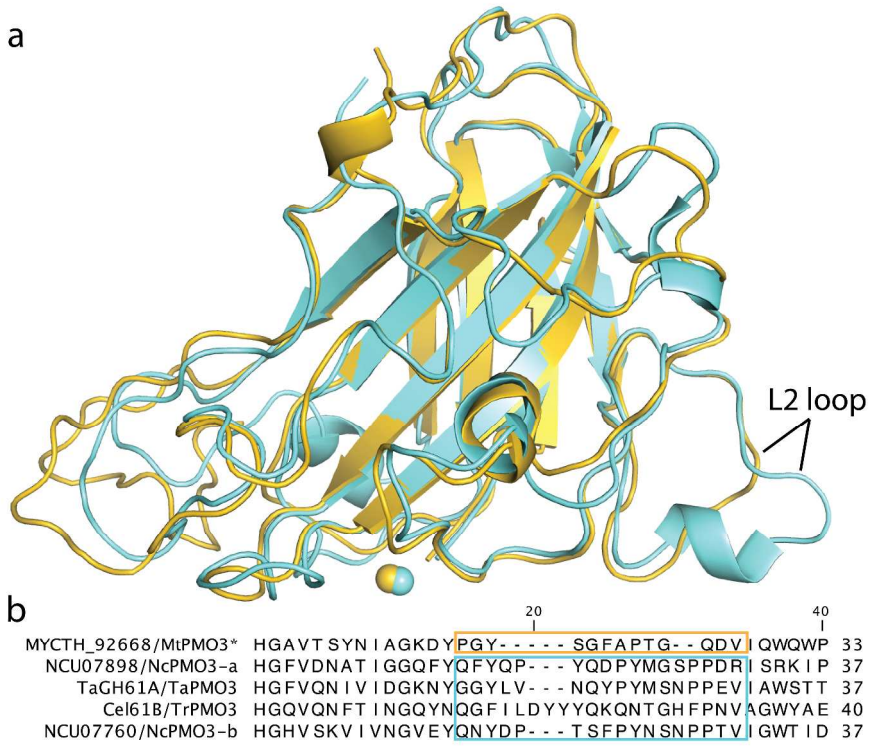

Supplementary Figure 4. (**a**) *Mt*PMO3* structure (yellow) superposed with *Nc*PMO3 (cyan, PDB ID 4EIS). Overall C_α RMSD ~ 0.8 Å (over 154 aligned residues). (**b**) Multiple sequence alignment of the first 40 residue positions of *Mt*PMO3* with four PMO3 sequences. The L2 loop sequences are highlighted with boxes. *Mt*PMO3* contains an abbreviated L2 loop that lacks α-helical structure compared with that of PMO3 enzymes.